Desalination and Water Treatment
www.deswater.com
doi: 10.1080/19443994.2015.1106982

57 (2016) 20069–20075
September

Taylor & Francis
Taylor & Francis Group

Synthesis and investigation of photocatalytic properties of Au/Fe_3O_4 nanocomposite materials for degradation of methylene blue

Asif Mahmood[a,*], Shahid Mahmood Ramay[b], Yousef S. Al-Zaghayer[a,c], Abdul-Aziz N. AlHazaa[b], Waheed A. Al Masary[a], Shahid Atiq[d]

[a]*Department of Chemical Engineering, College of Engineering, King Saud University, Riyadh, Saudi Arabia, Tel. +966 11 46 79966; Fax: +996 11 46 78770; email: ahayat@ksu.edu.sa (A. Mahmood), Tel. +966 11 46 76855; email: yszs@ksu.edu.sa (Y.S. Al-Zaghayer), Tel. +966 11 46 76853; email: walmasry@ksu.edu.sa (W.A. Al Masary)*
[b]*Department of Physics and Astronomy, Colleges of Science, King Saud University, Riyadh, Saudi Arabia, Tel. +966 11 4678760; email: smramay@yahoo.com (S.M. Ramay), Tel. +966 11 46 76640; email: aalhazaa@ksu.edu.sa (A.-A.N. AlHazaa)*
[c]*Supervisor of Industrial Catalysts Research Chair, King Saud University, Riyadh 11421, Saudi Arabia*
[d]*Centre of Excellence in Solid State Physics, University of the Punjab, New Campus, Lahore 54590, Pakistan, Tel. +92 300 7110532; email: shahidatiqpasrur@yahoo.com*

Received 8 April 2015; Accepted 23 September 2015

ABSTRACT

In this work, Au/Fe_3O_4 nanocomposite materials with exact spinel structure were successfully synthesized where impurities-free Fe_3O_4 was prepared using sol–gel auto-combustion method and gold was doped with various concentrations 1, 3, and 5 wt.% using conventional deposition–precipitation method. Methylene blue with fixed concentration (0.05 mM) was used to investigate the photocatalytic activity under visible light. Due to homogeneous and controlled compositions, Au/Fe_3O_4 nanocomposites showed enhanced photocatalytic efficiency than pure Fe_3O_4.

Keywords: Single-phase Fe_3O_4; Composite materials; Au nanoparticles; Photocatalytic activity; Methylene blue

1. Introduction

Recently, iron oxide magnetic nanoparticles (Fe_3O_4 MNPs) have been emphasized because of their surface areas and significant applications in a variety of fields such as wastewater purification [1], catalyst [2], magnetic resonance imaging [3,4], magnetic drug delivery [5], magnetic storage media [6], and photocatalyst [7]. Thus, a well-organized, rewarding, scalable, and non-hazardous fabrication of Fe_3O_4 MNPs is extremely insisted for forthcoming applications and fundamental research. However, to fabricate pure Fe_3O_4 powder having particular characteristics such as large surface area, small particle size, narrow size distribution, and excellent magnetic properties is a convoluted assignment [8].

Fe_3O_4 MNPs have been extensively applied in catalysis support, magnetic resonance imaging, adsorption, and environmental remediation, etc. [9]. Fe_3O_4 MNPs in photocatalysis process have attracted considerable attention due to their high efficiency, good stability, availability, and non-toxicity [7]. Their resultant samples reveal better photodegradation

*Corresponding author.

ability and can be easily recycled by applying an external magnetic field.

Among the nanostructured materials, gold nanoparticles (AuNPs) have received remarkable consideration in recent years due to fabulous stability, biocompatibility, surface plasmon resonance effect, and exceptional catalytic activities [10]. The marvelous catalytic properties of the catalysts with gold have been achieved in many reactions of both industrial and environmental importance. Dimensions of gold particles [10–15], material used as support, the synthesis method, fabrication conditions, and catalyst activation procedure [16,17] are the effective parameters to enhance the catalytic activity.

In this work, we prepared a novel nanocomposite of Au/Fe_3O_4 by doping AuNPs on Fe_3O_4 using deposition precipitation method. Au/Fe_3O_4 nanocomposite is extensively valid for various applications such as wastewater purification, magnetic drug delivery, bioseparation. However, only immaterial research has been carried out so far using Au/Fe_3O_4 as a photocatalyst. In view of fulfilling this research deficiency, we have fabricated Fe_3O_4 with/without gold doping with different concentrations of gold (1, 3, and 5 wt.%) to study the photocatalytic activity by evaluating the degradation of aqueous solution of methylene blue (MB) under visible light under the full control of parameters.

The objective of this study was to prepare Fe_3O_4 with/without gold doping catalysts to study their catalytic performance and stability as a function of time for the degradation of the MB in water under visible light. In this work, we prepared a new nanocomposite of Fe_3O_4 with/without gold doping by reacting Fe_3O_4 with AuNPs, and sample having 5 wt.% Au concentration exhibited an additional enhancement in the catalytic activity.

2. Experimental section

2.1. Materials

99.99% pure iron nitrate ($Fe(NO_3)_3{\cdot}9H_2O$), 99% pure glycine (NH_2CH_2COOH), 98% pure NaOH, deionized water (H_2O) from Sigma-Aldrich, AuCl (Acros), and MB ($C_{16}H_{16}ClN_3S_4{\cdot}xH_2O$) from Qualikems Fine Chem. Pvt. Ltd were procured and were used without any additional treatment.

2.2. Preparation of Fe_3O_4

Fe_3O_4 powder was prepared using iron nitrate as a precursor powder via sol–gel auto-combustion method where glycine was used as a fuel agent. The aqueous solution of precursor powder was prepared in 50 ml of deionized water. A brownish color xerogel was collected by centrifugation, dried in furnace at 400˚C for 2 h.

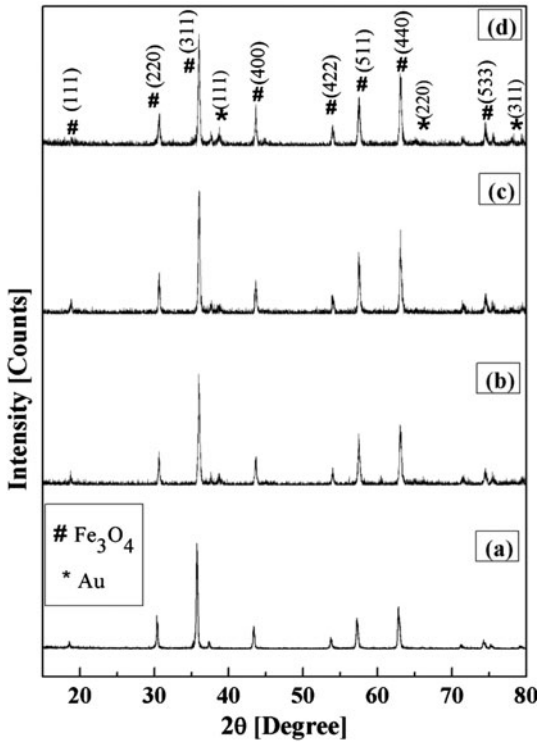

Fig. 1. XRD patterns of samples (a) Fe_3O_4, Au-doped Fe_3O_4, (b) 1 wt.%, (c) 3 wt.%, and (d) 5 wt.%.

2.3. Au doping on Fe_3O_4 powder

1, 3, and 5 wt.% gold was doped using conventional deposition–precipitation method. The detailed doping procedure and experimental conditions were described somewhere else [10].

2.4. Characterizations

The crystalline phase and size of all the samples of Fe_3O_4 powder with/without gold doping were analyzed by X-ray diffractometer (XRD) which were carried out at a Rigaku Ultima iv with Cu Kα radiations (λ = 1.5406 Å) from 15˚ to 80˚ in 0.01˚ increments. Scanning electron microscopy (SEM) images were carried out at a SEM, JEOL JSM-7600F, FESM, Japan. Transmission electron microscopy (TEM) was carried out at a JEOL 2100F, FEG-TEM Japan. Diffuse reflection and absorbance spectra were measured using

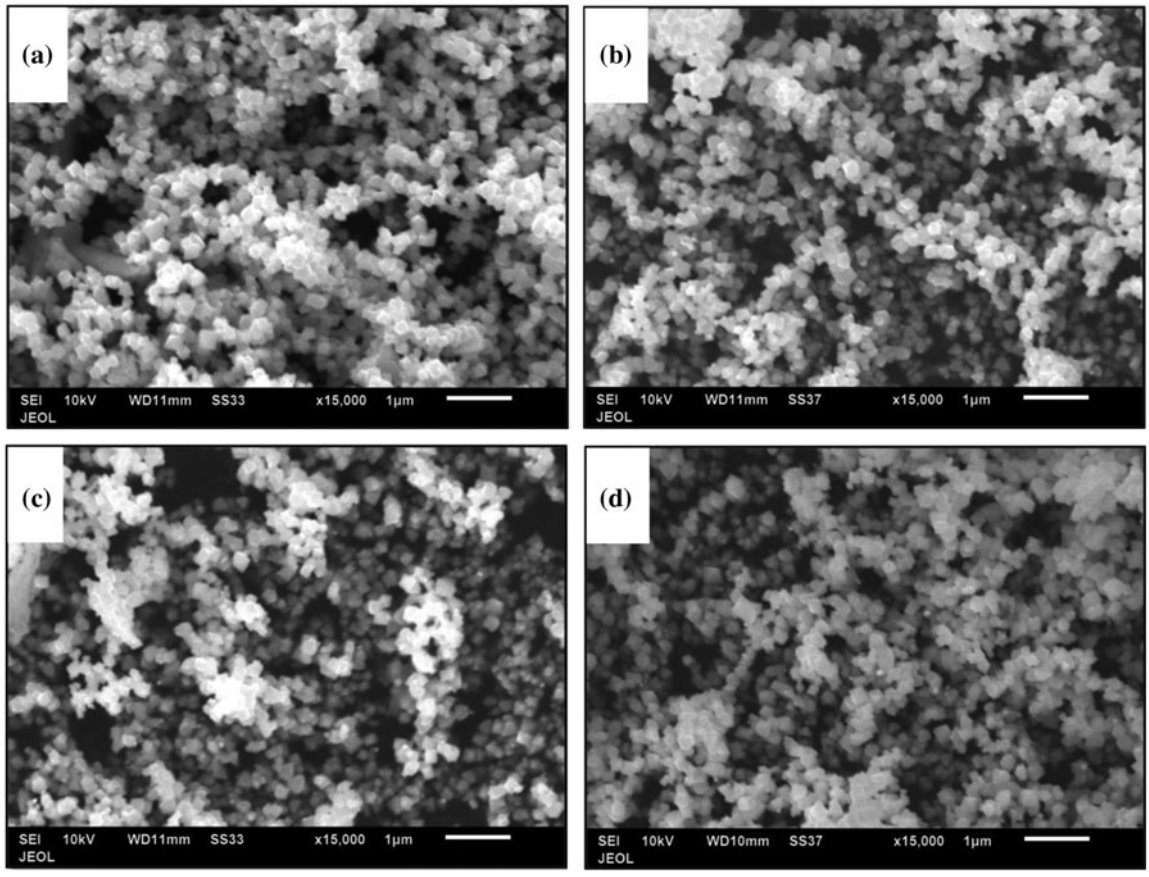

Fig. 2. SEM micrographs of samples (a) Fe_3O_4, Au-doped Fe_3O_4, (b) 1 wt.%, (c) 3 wt.%, and (d) 5 wt.%.

PerkinElmer's LAMBDA 35 and Labomed-2950, USA spectrophotometers, respectively.

3. Results and discussion

3.1. Characterizations

3.1.1. XRD analysis

Fig. 1 elucidates the XRD patterns of with/without gold-doped Fe_3O_4 composite materials where the formation of single-phase Fe_3O_4 powder can be observed. The crystal structures are well agreed with the corresponding reported JCPDS data (JCPDS card No. 79-0418). All the diffraction peaks from 15° to 80° scan can be indexed as (1 1 1), (2 2 0), (3 1 1), (4 0 0), (4 2 2), (5 1 1), (4 4 0), and (5 3 3) planes of the Fe_3O_4 crystals (Fig. 1(a)–(d)).

Furthermore, the presence of metallic gold peaks can be observed in the Fig. 1(b)–(d) which are well agreed with the corresponding reported JCPDS data (JCPS card no. 00-004-0784). Metallic gold peaks were examined at $2\theta = 44.39°$, 64.57°, and 77.54° in all the gold-doped samples (Fig. 1(b)–(d)).

3.1.2. SEM analysis

Fig. 2(a)–(d) shows the SEM images of all the samples of Fe_3O_4 powder with/without gold doping. Further, elemental analysis was done by attached EDS analysis (Oxford instruments, UK).

The regular spherical shape particles with a very small diameter of 20 nm were observed in the SEM picture. Fig. 2(b)–(d) revealed the particle size of Fe_3O_4 that was not too much affected by gold doping.

Fig. 3 shows energy dispersive X-ray spectroscopy (EDX) analysis that revealed characteristic peaks for the presence of Au, Fe, and O in Au/Fe_3O_4 composite material.

3.1.3. TEM analysis

Particles size, distribution of particles, and shape of Au/Fe_3O_4 composite material were examined by TEM. Fig. 4(d) displayed the 5 wt.% Au sample which showed more population of the particles on the surfaces of Fe_3O_4 than other samples. Fig. 4(d) showed that each iron oxide particle attracts about 10–15 Au particles on its surface.

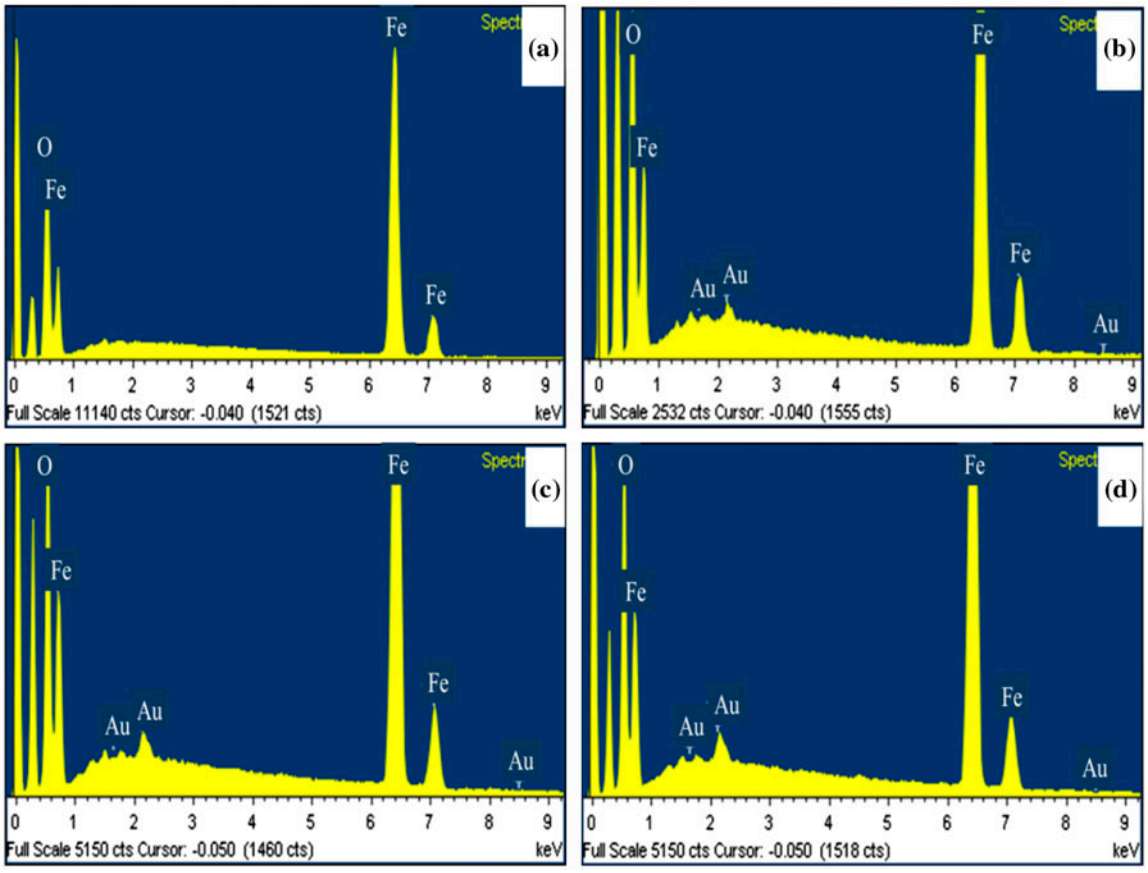

Fig. 3. EDX of samples (a) Fe_3O_4, Au-doped Fe_3O_4, (b) 1 wt.%, (c) 3 wt.%, and (d) 5 wt.%.

Further analysis was done using high-resolution transmission electron microscopy as shown in Fig. 5 where HR-TEM analysis further validate the size confinement of the Au particles. Single-phase nature of both particles confirm due to the correspond of lattice fringes to atomic planes within particle.

3.2. Photocatalytic properties

3.2.1. Reflectance spectra

Fig. 6 illustrates the reflectance spectra of Fe_3O_4 with/without Au doping. The peaks show the weak reflectance for Fe_3O_4. For comparison, Fe_3O_4 with/without Au-doped samples have almost reflectance in the same wavelength region. However, with an increase in the Au contents, there is small redshift in the characteristic peak. The Fe_3O_4 sample without Au doping shows a characteristic peak around 532 nm (Fig. 6(a)); however, 5 wt.% Au-doped Fe_3O_4 sample shows a characteristic peak around 538 nm (Fig. 6(d)). 5 wt.% Au-doped sample presents redshifts reflection peak by 6 nm with respect to that of the Fe_3O_4 without Au doped. This redshift is a result of the decoration of the Fe_3O_4 by the doped Au particles.

There is a noticeable peak shift in the reflection spectra (Fig. 6(a)–(d)). Due to decrease in wavelength from 532 to 538 nm, band gap energy of Au-doped Fe_3O_4 nanocomposites decrease as well. It may be assumed that band shrinkage effect can cause the reduction in band gap that happen due to Au doping on Fe_3O_4 [18].

3.2.2. Absorbance spectra

Fig. 7 shows the absorption spectra of the degraded MB solutions with respect to light exposure. The absorption spectra were taken after 45 min for each sample, revealed that the Fe_3O_4 sample without Au doping showed poor photocatalytic activity (Fig. 7(a)). This may be due to the fast recombination of generated charge carriers on the long migration route to the surface of Fe_3O_4 nanoparticles [19].

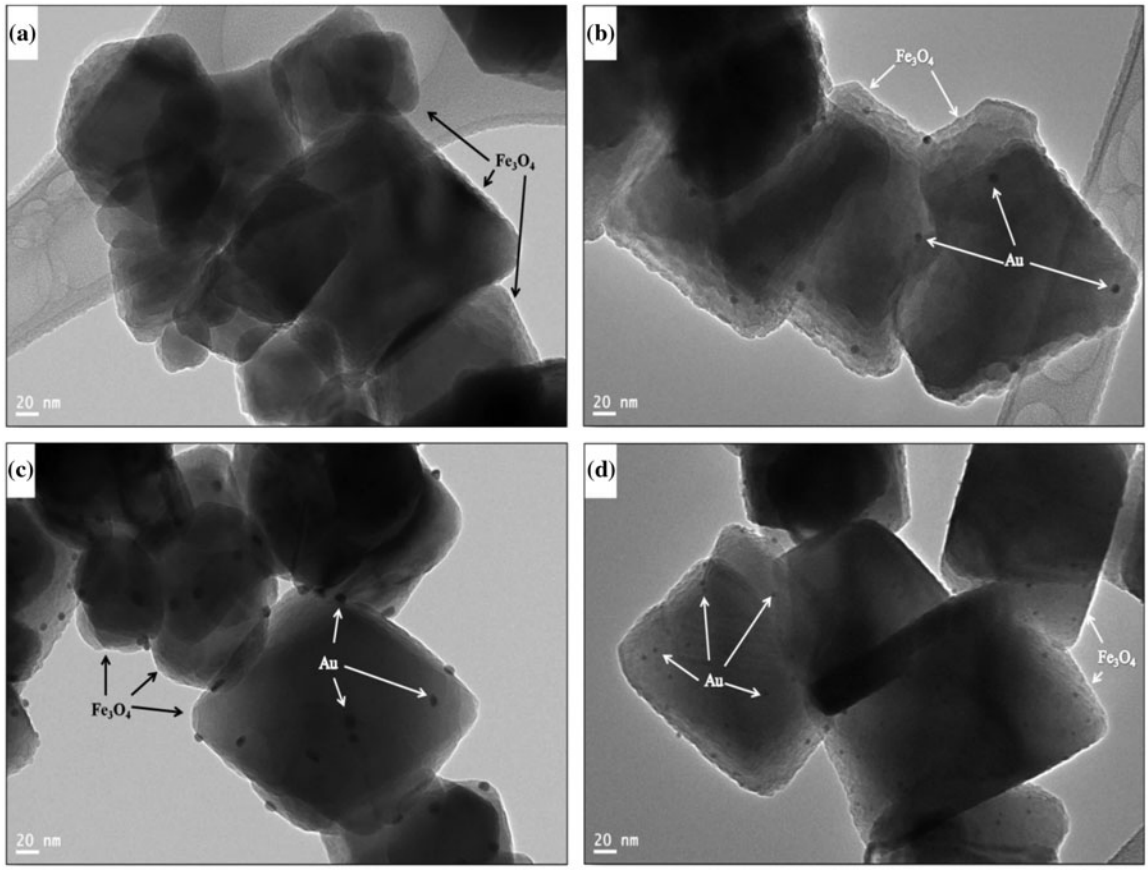

Fig. 4. TEM images of samples (a) Fe_3O_4, Au-doped Fe_3O_4, (b) 1 wt.%, (c) 3 wt.%, and (d) 5 wt.%—indicating the attachment of Au nanoparticles (white arrows) on Fe_3O_4.

It is clearly noticeable that the doping of Au contents has a real impact on the absorption of MB. Fig. 7(d) revealed this observation where Fe_3O_4 samples having 5 wt.% Au showed high degradation after 45 min under visible light (Fig. 7(d)). It can be examined that the absorbance at 662 nm (for Fe_3O_4 sample without Au doped) rapidly decreases compare to the sample having Au doping. These outcomes verified the improved photocatalytic activity of the Fe_3O_4 sample having Au under visible light compared to the Fe_3O_4 sample having no gold. Such kind of improvement in the photocatalytic activity can be endorsed to the tremendous electronic conductivity and improved mass transportation, which helps photoinduced electron movement to the surface of catalysts, which can reduce the recombination of both photoinduced electrons and holes [19]. Furthermore, the results also showed an attractive sequence of improved photocatalytic activity of all Fe_3O_4 with/without Au doping. The order for MB degradation of Fe_3O_4 with/without Au doping showed MB degradation for 5 wt.% Au/Fe_3O_4 > 3 wt.% Au/Fe_3O_4 > 1 wt.% Au/Fe_3O_4 > Fe_3O_4 (without Au doping).

This sequence of degradation exactly follows the order of reflection spectra trend obtained for all samples. The redshift in reflection spectra by an increase in Au contents in the sample exhibits the effectiveness of the Au-doped catalysts for MB degradation in the visible light. Finally, it may be concluded that increased Au contents in pure Fe_3O_4 can cause the reduction of band gap and enhance the active sites thus improved the quality of the fabricated samples, which was confirmed experimentally by assessing the degradation of MB in the presence of fabricated catalysts. However, excess of Au cover the Fe_3O_4 surface, thus hindering the hollow lattices which decreases the surface area of the catalysts and finally lowers the photocatalytic activity [20]. Therefore, only appropriate amount of Au were doped to get superior photocatalytic properties.

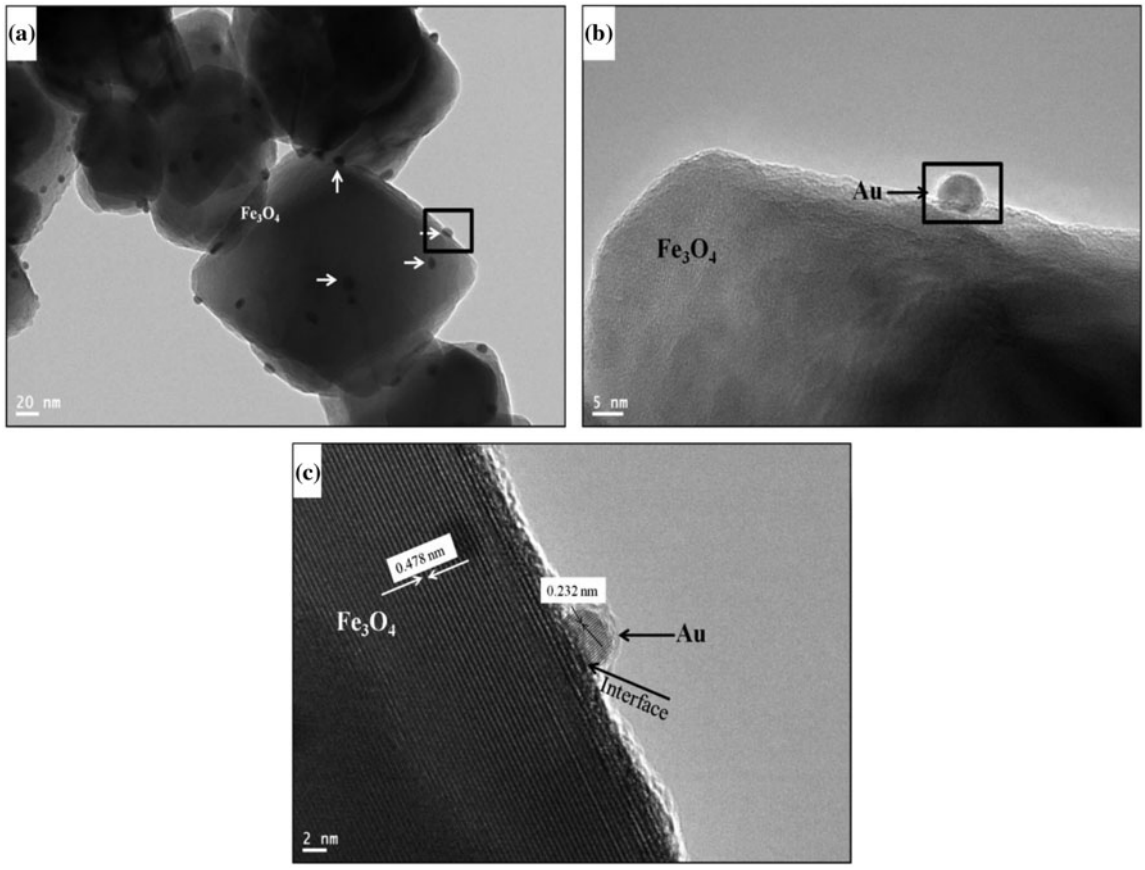

Fig. 5. HR-TEM images of (3 wt.% Au-doped Fe_3O_4) Au nanoparticle (as shown with the help of box) attahed with Fe_3O_4 surafce and lattice-resolved HR-TEM image of the Au nanoparticle and Fe_3O_4 crystal interface is very clear.

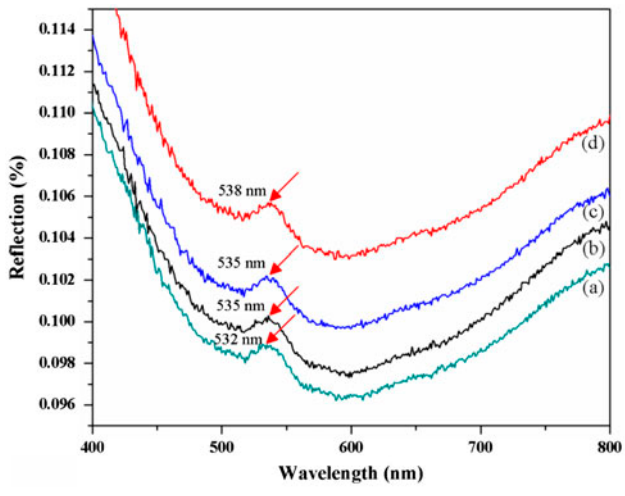

Fig. 6. Reflection spectra measured for sample (a) Fe_3O_4, Au-doped Fe_3O_4, (b) 1 wt.%, (c) 3 wt.%, and (d) 5 wt.%.

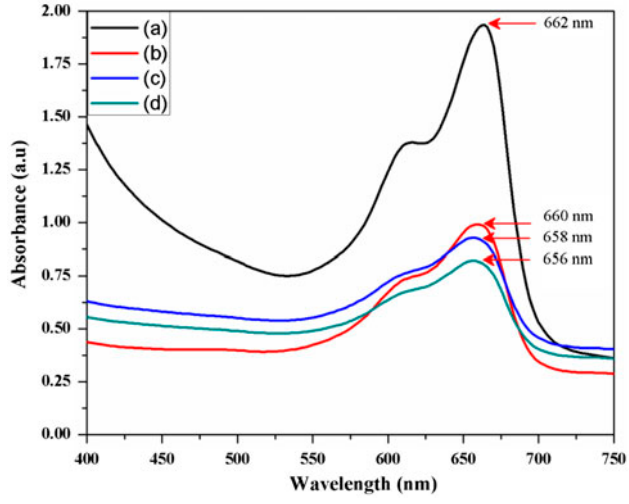

Fig. 7. Time-dependent absorption spectra of (a) Fe_3O_4, Au-doped Fe_3O_4, (b) 1 wt.%, (c) 3 wt.%, and (d) 5 wt.%.

4. Conclusions

Single-phase Fe_3O_4 and Au/Fe_3O_4 nano composites were successfully synthesized via sol–gel auto-combustion and conventional deposition–precipitation techniques, respectively, to investigate the degradation of MB under visible light. The results showed that the synthesized composite materials have excellent photocatalytic activity. 5 wt.% Au-doped sample was found to display superior photocatalytic activity than Fe_3O_4 sample without Au doping.

Acknowledgment

The authors extend their appreciation to the Deanship of Scientific Research at King Saud University for funding the work through the research group project no. RGP-VPP-106.

References

[1] Y.F. Shen, J. Tang, Z.H. Nie, Y.D. Wang, Y. Ren, L. Zuo, Preparation and application of magnetic Fe_3O_4 nanoparticles for wastewater purification, Sep. Purif. Technol. 68 (2009) 312–319.
[2] S. Kim, E. Kim, B.M. Kim, Fe_3O_4 nanoparticles: A conveniently reusable catalyst for the reduction of nitroarenes using hydrazine hydrate, Chem. Asian J. 6 (2011) 1921–1925.
[3] G. Zhao, J. Wang, X. Peng, Y. Li, X. Yuan, Y. Ma, Facile solvothermal synthesis of mesostructured Fe_3O_4/chitosan nanoparticles as delivery vehicles for pH-responsive drug delivery and magnetic resonance imaging contrast agents, Chem. Asian J. 9 (2014) 546–553.
[4] G. Wang, G. Chen, Z. Wei, X. Dong, M. Qi, Multifunctional Fe_3O_4/graphene oxide nanocomposites for magnetic resonance imaging and drug delivery, Mater. Chem. Phys. 141 (2013) 997–1004.
[5] F.H. Chen, L.M. Zhang, Q.T. Chen, Y. Zhang, Z.J. Zhang, Synthesis of a novel magnetic drug delivery system composed of doxorubicin-conjugated Fe_3O_4 nanoparticle cores and a PEG-functionalized porous silica shell, Chem. Commun. 46 (2010) 8633–8635.
[6] M. Abbas, B.P. Parvatheeswara Rao, S.M. Naga, M. Takahashi, C. Kim, Synthesis of high magnetization hydrophilic magnetite (Fe_3O_4) nanoparticles in single reaction—Surfactantless polyol process, Ceram. Int. 39 (2013) 7605–7611.
[7] R. Wang, X. Wang, X. Xi, R. Hu, G. Jiang, Preparation and photocatalytic activity of magnetic $Fe_3O_4/SiO_2/TiO_2$ composites, Adv. Mater. Sci. Eng. 2012 (2012) 409379.
[8] R. Ianoş, A.T. Culescu, C.P. Curariu, I. Lazau, Solution combustion synthesis and characterization of magnetite, Fe_3O_4, nanopowders, J. Am. Ceram. Soc. 95 (2012) 2236–2240.
[9] X. Yang, Z. Tan, Y. Fu, G. Li, H. Xu, Synthesis and characterization of Au/Fe_3O_4 nano-composite, Adv. Mater. Res. 1082 (2015) 6–9.
[10] A. Mahmood, S.I. Woo, Enhancement of catalytic activity of Au/TiO_2 by thermal and plasma treatment, Korean J. Chem. Eng. 30 (2013) 1876–1881.
[11] G.C. Bond, D.T. Thompson, Catalysis by gold, Catal. Rev. Sci. Eng. 41 (1999) 319–388.
[12] M. Haruta, When gold Is not noble: Catalysis by nanoparticles, Chem. Record 3 (2003) 75–87.
[13] R. Zanella, S. Giorgio, C.H. Shin, C.R. Henry, C. Louis, Characterization and reactivity in CO oxidation of gold nanoparticles supported on TiO_2 prepared by deposition–precipitation with NaOH and urea, J. Catal. 222 (2004) 357–367.
[14] I. Laoufi, M.C. Saint-Lager, R. Lazzari, J. Jupille, O. Robach, S.G.G. Garaudée, G. Cabailh, P. Dolle, H. Cruguel, Size and catalytic activity of supported gold nanoparticles: An in operando study during CO oxidation, J. Phys. Chem. C 115 (2011) 4673–4679.
[15] R. Gonz, V. Zanella, R. del-Angel, R.G. Gomez, MTBE visible-light photocatalytic decomposition over Au/TiO_2 and Au/TiO_2–Al_2O_3 sol–gel prepared catalysts, J. Mol. Catal. A 281 (2008) 93–98.
[16] M. Haruta, Size- and support-dependency in the catalysis of gold, Catal. Today 36 (1997) 153–166.
[17] J.D. Grunwaldt, C. Kiener, C. Wögerbauer, A. Baiker, Preparation of supported gold catalysts for low-temperature CO oxidation via "size-controlled" gold colloids, J. Catal. 181 (1999) 223–232.
[18] A. Mahmood, S.M. Ramay, Y.S. Al-Zaghayer, S. Atiq, I. Ahmad, M.A. Shar, S.D. Khan, Study the structure and performance of thermal/plasma modified Au nanoparticle-doped TiO_2 photocatalyst, Mod. Phys. Lett. B 28 (2014) 1450208, 12 pp.
[19] Y.H. Kim, H.C. Choi, ZnO on thiolated graphene oxide as efficient photocatalyst for degradation of methylene blue, Bull. Korean Chem. Soc. 34 (2013) 3586–3590.
[20] Y.L. Lai, M. Meng, Y.F. Yu, One-step synthesis, characterizations and mechanistic study of nanosheets-constructed fluffy ZnO and Ag/ZnO spheres used for Rhodamine B photodegradation, Appl. Catal. B: Environ. 100 (2010) 491–501.